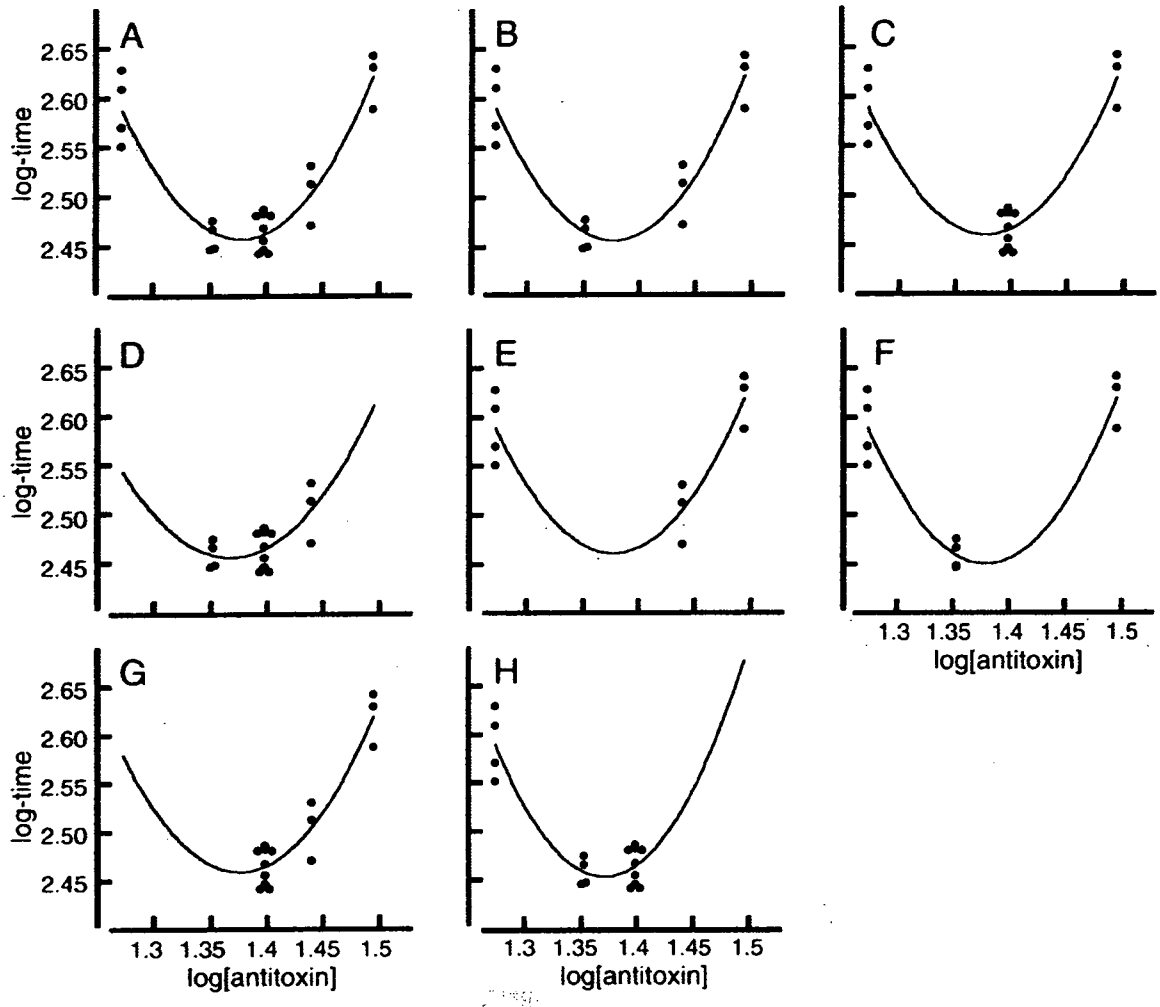

Fig. 2. Parabolic regression curves for flocculation assays of diphtheria toxoid at the 25 Lf/ml level. Time required to reach a particle count of 50,000 was extracted from recorded data for Dtd A at the 25 Lf/ml level and plotted. Raw data and parabolic regression curves are shown. A (5 data points), data and regression curve from assays using 18.75, 22.5, 25, 27.5 and 31.25 units/ml of antitoxin and approximately 25 Lf/ml of toxoid. B (4 data points), 18.75, 22.5, 27.5 and 31.25 units/ml of antitoxin. C (3 data points), 18.75, 25 and 31.25 units/ml of antitoxin. D (3 data points), 22.5, 25 and 27.5 units/ml of antitoxin. E (3 data points), 18.75, 27.5 and 31.25 units/ml of antitoxin. F (3 data points), 18.75, 22.5 and 31.25 units/ml of antitoxin. G (3 data points), 25, 27.5 and 31.25 units/ml of antitoxin. H (3 data points), 18.75, 22.5 and 25 units/ml of antitoxin.

Fig. 1E shows the results of 50 Lf/ml level assays carried out with Dtd from another manufacturer (Dtd B) with 37.5, 50 and 62.5 units/ml, again showing quantitative properties with clear differences between the three curves. Similarly, Ttd from manufacturer A (Ttd A) and the Japanese reference tetanus antitoxin for flocculation at the 50 Lf/ml level exhibited different curve patterns depending on antitoxin content. The time needed before the initiation of flocculation was longer than in the case of diphtheria toxoid (Fig. 1F).

3.3. Statistical analyses

In order to investigate the reliability of the light scattering assays and to establish a quantitative system, further measurements were done on Dtd A and the results were rigorously analyzed using statistical methods. The measurements, including those described above, were done with 18.75, 22.5, 25, 27.5 and 31.25 units/ml of antitoxin for 25 Lf/ml level assays and 37.5, 45, 50, 55 and 62.5 units/ml of antitoxin for 50 Lf/ml level assays, as depicted in Fig. 1B and D, respectively. The measurements were repeated nine times for 25 units/ml, four times each for 18.75 and 22.5 and three times each for 27.5 and 31.25 units/ml for 25 Lf/ml level assays. For assays at the 50 Lf/ml level, measurements were repeated eight times for 50 units/ml and three times each for the other concentrations. From the data, the time required for reaching particle counts of 10,000, 20,000, 50,000, 100,000 and 150,000 were extracted and log-transformed for further analysis. Bartlett's test showed that homogeneity of variance was generally attained for the groups of repeated particle counts for each antitoxin dose (data not shown). Log-

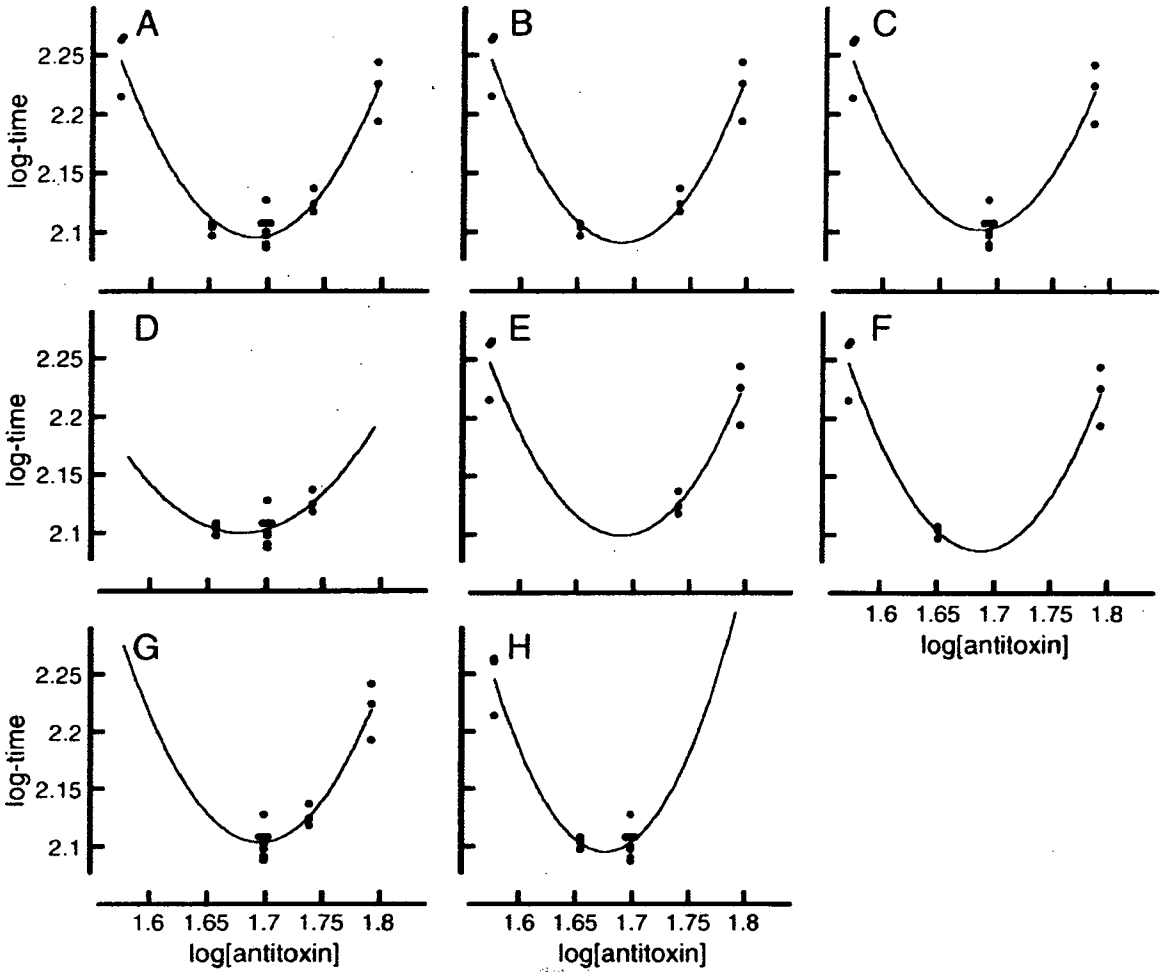

Fig. 3. Parabolic regression curves for flocculation assays of diphtheria toxoid at the 50 Lf/ml level. Raw data at the 50 Lf/ml level assays for Dtd A and parabolic regression curves are shown. A (5 data points), data and regression curve from assays using 37.5, 45, 50, 55 and 62.5 units/ml of antitoxin and approximately 50 Lf/ml of toxoid. B (4 data points), 37.5, 45, 55 and 62.5 units/ml of antitoxin. C (3 data points), 37.5, 50 and 62.5 units/ml of antitoxin. D (3 data points), 45, 50 and 55 units/ml of antitoxin. E (3 data points), 37.5, 55 and 62.5 units/ml of antitoxin. F (3 data points), 37.5, 45 and 62.5 units/ml of antitoxin. G (3 data points), 50, 55 and 62.5 units/ml of antitoxin. H (3 data points), 37.5, 45 and 50 units/ml of antitoxin.

time data for 50,000 counts of both 25 and 50 Lf/ml level assays were plotted against log[antitoxin] as examples (Figs. 2A and 3A). The Lf measurement is based on the fact that the fastest flocculation takes place for the mixture of toxoid and antitoxin at the most appropriate ratio and a parabolic curve has been proposed to represent the time required for forming of visible toxoid–antitoxin complex for varied antitoxin

Table 2
Deviation from quadratic regression curves in light scattering assays for diphtheria toxoid from manufacturer A

		Deviation from quadratic equation at threshold particle count of				
		10,000	20,000	50,000	100,000	150,000
25 Lf/ml level[a]	Variance	2.49×10^{-4}	9.33×10^{-5}	2.98×10^{-4}	3.47×10^{-4}	4.03×10^{-4}
	Error	6.51×10^{-4}	5.89×10^{-4}	5.66×10^{-4}	7.07×10^{-4}	1.31×10^{-3}
	F value	0.382	0.158	0.526	0.491	0.307
50 Lf/ml level[b]	Variance	2.06×10^{-4}	1.39×10^{-4}	1.88×10^{-4}	2.82×10^{-4}	3.78×10^{-4}
	Error	4.33×10^{-4}	2.87×10^{-4}	2.64×10^{-4}	2.93×10^{-4}	3.66×10^{-4}
	F value	0.476	0.484	0.711	0.965	1.031

[a] Calculated from results of assays containing 18.75 ($n=4$), 22.5 ($n=4$), 25 ($n=9$), 37.5 ($n=3$) and 31.25 ($n=3$) units/ml of antitoxin.
[b] Calculated from results of assays containing 37.5 ($n=3$), 45 ($n=3$), 50 ($n=8$), 55 ($n=3$) and 62.5 ($n=3$) units/ml of antitoxin.

Table 3
Estimated Lf values by different methods of sampling in light scattering assays for diphtheria toxoid from manufacturer A

	Estimated Lf values by assays using datapoints of							
	5 doses[a]	4 doses[b]	3 doses-1[c]	3 doses-2[d]	3 doses-3[e]	3 doses-4[f]	3 doses-5[g]	3 dose-6[h]
25 Lf/ml level	190.8	191.0	191.1	186.8	191.1	191.3	190.2	187.8
50 Lf/ml level	195.8	195.7	196.2	189.6	196.1	195.9	198.6	189.7

[a] [h] corresponds to Figs. 2 and 3 panel A to H, respectively.

concentrations in the flocculation assay (Levine and Wyman, 1965; Lyng and Bentzon, 1987). Accordingly, a quadratic regression analysis was carried out to fit an equation to the relation of log[antitoxin] and log-time for reaching 50,000 counts (Figs. 2A and 3A). Calculated F-values showed that deviation of the log-time data from the parabolic regression curve was small enough for all threshold particle counts (Table 2). The Lf value, therefore, could be calculated as the local minimum of the parabolic curve.

To examine possible simplifications of the test, various combinations of antitoxin concentrations and log-time data were selected from repeated measurements described above to construct data sets of smaller numbers of doses and repetitions to calculate corresponding Lf values.

Parabolic curves were fitted to the data sets constructed from a reduced number of doses by the quadratic regression analysis, and the results on the selected data sets of assays at the threshold of 50,000 particle counts are depicted in Figs. 2B–H and 3B–H for 25 and 50 Lf/ml level assays, respectively. Lf values calculated for the data sets in Figs. 2 and 3 are summarized in Table 3. Calculated Lf values agree well with the values from observations by eye. Values calculated by the four-dose results (b) were shown to be consistent with the five-dose results (a). Three-dose results also yielded consistent results for Lf estimation comparable to the five-dose results provided that the doses were selected so that the expected value of Lf was included within the range (Figs. 2 and 3C–G). This suggests the feasibility of three-dose assays.

Reproducibility of the light-scattering flocculation assay with fewer repeated measurements was assessed. The data selection for repeats was done in the following way: 1) for doses with not more than triplicate measurements, all data were selected, 2) for doses with data from quadruplicate or more measurements, the maximum value, the minimum value and a median value (or an average of median values) were selected. All possible combinations of duplicated data for each five-dose assay were generated from the results of five-dose assays at the 50 Lf level and 25 Lf level of Dtd to construct $3^5=243$ data sets (two among three data points each for five doses) for each Lf level. Each of the selected data sets was fitted with a quadratic equation to calculate Lf values, and reproducibility of Lf estimation was assessed as the extent of variance of log-Lf values. Similar analyses were carried out for all threshold particle counts for both 25 Lf and 50 Lf levels and the results are summarized in Table 4. Lf values calculated for all possible data sets of two repeated measurements for five doses showed very small variation, as seen in Table 4.

As the light-scattering flocculation assay was shown to have excellent precision, the possibility of simplifying the assay was examined by further reducing the data set from 5 doses to 3 doses, and by reducing the repeat number to duplicate or single assays. Similar to the above-mentioned data sets, single or duplicated data were generated for three or five doses of antitoxin. Selected data sets were then fitted with quadratic equations to calculate Lf values. Reproducibility of the Lf assessments was compared as differences in the magnitude of variation between three-dose and five-dose assays and also between single and duplicate measurements. Variance of log(estimated Lf), calculated from the data at 50 Lf/ml level at the threshold count of

Table 4
Variance of estimated Lf values in light scattering assays for diphtheria toxoid from manufacturer A

	Variance of log(estimated Lf) at threshold particle count of				
	10,000	20,000	50,000	100,000	150,000
25 Lf/ml level[a] ($n=243$)	5.90×10^{-6}	7.06×10^{-6}	7.18×10^{-5}	4.05×10^{-5}	5.87×10^{-6}
50 Lf/ml level[a] ($n=243$)	2.83×10^{-6}	4.00×10^{-6}	3.93×10^{-6}	1.61×10^{-6}	7.60×10^{-6}

[a] Performed by selecting all possible random combinations of data points as described in the text.

50,000, for example, indicated that variation of log-Lf values for five-dose assays was comparable with or 1.5 times smaller than that for three-dose assays (for single measurements, 3.69×10^{-5} at 5 doses vs. 5.79×10^{-5} at 3 doses; for duplicate measurements, 7.42×10^{-6} at 5 doses vs. 1.20×10^{-5} at 3 doses). In contrast, the above data indicate that reducing the number of measurements from duplicate to single decreased reproducibility approximately 4.8 times.

4. Discussion

In the present study, we have described a novel detection system for toxoid flocculation assays, using a laser light-scattering platelet aggregometer. The system provides a highly reproducible, quantitative toxoid flocculation assay, giving statistically acceptable results provided that at least three doses of antitoxin against one fixed dose of toxoid are employed in duplicate measurements.

As the Lf value has been practically the only measure to assess and label antigen content of toxoid products to date, determination of Lf values is an indispensable tool for quality control of toxoid vaccines, as well as toxins and antitoxins themselves. However, methods for the determination of Lf values have remained essentially unchanged since their first description in 1922 (Ramon, 1922b,a). The method, employing observation by eye for detecting initiation of flocculation, has the disadvantage of low reproducibility due to a large person-to-person variation (compare Kf values for observers 1 and 2 in Table 1). In order to overcome these problems, we constructed a novel flocculation assay system using a laser light-scattering platelet aggregometer as a detector. As shown in Fig. 1A and C, excellent reproducibility could be achieved with this method.

Because the resolution of the human eye differs between individual observers and is generally not better than 20–40 μm (Künzel et al., 2003), the aggregometer system with a resolution of 9 μm can provide more rapid detection. In fact, the Kf values by observation by eye presented in Table 1 were approximately 9 to 10 min. The laser light-scattering detection device needed a shorter time, so that even when measuring 150,000 particle counts, the assay finished within 8 min for a 25 Lf/ml level of Dtd. Assays at lower threshold particle counts can be finished in a shorter time.

A parabolic regression curve could be fitted to the relation of the logarithm of time required to reach a specific particle count (log-time) and the logarithm of antitoxin concentration (log[antitoxin]), according to quadratic regression analysis. The antitoxin concentration giving the minimum log-time could be estimated as the local minimum of the parabolic curve. The fit of the parabolic regression curve was satisfactory and the calculated Lf values were highly reproducible. Theoretical analyses on flocculation have been done by several groups (Bowen and Wyman, 1953b,a; Boyd and Purnell, 1944; Lyng and Bentzon, 1987). Lyng and Bentzon (1987) showed, from their results, that log-time fits to a function of log([antitoxin]×[toxoid]) and log([toxoid]/[antitoxin]) in the equation

$$y = b_0 + b_1x + b_2z + b_3x^2 + b_4z^2 + b_5xz$$

where

x log([toxoid]×[antitoxin])=log([toxoid])+log([antitoxin])
y log-time
z log([toxoid]/[antitoxin])=log([toxoid])−log([antitoxin]).

That is, when the product of concentrations ([toxoid]×[antitoxin]) is constant, parabolic regression could be applied between log-time and log([toxoid] / [antitoxin]). This had also been shown by Levine and Wyman in 1965 by comparing the results from three kinds of assays: (1) the Ramon (beta) method (Ramon, 1922c) which is still the most common method recommended in the WHO minimum requirements, in which the concentration of toxoid is set constant, (2) the Dean–Webb (alpha) method in which the concentration of antitoxin is set constant, and (3) the mass-law method (Levin and Wyman method) in which the product of concentrations of toxoid and antitoxin is set constant. Discrepancies between the estimated Lf values measured by the Ramon method and the Dean–Webb method had already been recognized (Bowen and Wyman, 1953b), and Levine and Wyman showed experimentally that the mass-law (Levine–Wyman) method would be ideal for parabolic regression (Levine and Wyman, 1965). In the present study, the Ramon method performed adequately and was employed throughout. The results were fitted with parabolic regression curves to allow highly reproducible estimations of Lf values (Tables 2–4). In addition, combinations of selected results to mimic single and duplicate assays showed that duplicate assays gave less variance of estimated Lf values compared to single assays. The analysis also showed that assays employing 3 different antitoxin concentrations resulted in similar levels of variance in estimated Lf values as 5-dose assays. This means that assays with 3 different doses of antitoxin are sufficient for reliable flocculation analysis.

The assay system was applicable not only to Dtd but also to Ttd measurements. Although statistical analyses were not done on the results from assays with tetanus toxoids, Ttd required a longer time for initiating the increase of particle counts (Fig. 1F). This result is consistent with the results of the conventional flocculation assay for the same Ttd, in which a longer time was needed for flocculation (Kf=approximately 19 min at 25 Lf/ml) compared to the results of Dtds at the same level illustrated in Table 1.

The aggregometer detects scattered light from particles in the reaction cuvette and particle size can be calculated from the observed light intensity (Ozaki et al., 1994; Yamamoto et al., 1995). Turbidimetric measurement of antigen–antibody reactions by detecting precipitin formation was reported previously (Jacobsen and Steensgaard, 1979). We also tried to apply the turbidimetric type of aggregometer to flocculation assays. However, the turbidimetric system was not capable of determining the most appropriate toxoid–antitoxin ratio (data not shown).

The results presented here show that this novel detection system has potential application for routine toxoid flocculation assays. Further calibration, if possible through international collaboration, could finally result in the establishment of a new routine method for toxoid flocculation assays.

Acknowledgements

We are grateful to the Kowa Company, Limited (Nagoya, Japan) for lending us the laser light-scattering platelet aggregometer PA-20, and are also grateful to The Research Foundation for Microbial Diseases of Osaka University (Biken) and Takeda Pharmaceutical Company Limited for diphtheria and tetanus toxoids. This study was supported by a Health and Labour Sciences Research Grant (Research on Regulatory Science of Pharmaceuticals and Medical Devices) from the Ministry of Health, Labour and Welfare of Japan.

References

Bowen, H.E., Wyman, L., 1953a. The flocculation reaction of rabbit antibody. J. Immunol. 71, 86.

Bowen, H.E., Wyman, L., 1953b. On the lack of agreement of the constant toxin and constant antitoxin flocculation reactions of diphtheria toxin and equine antitoxin. J. Immunol. 70, 235.

Boyd, W.C., Purnell, M.A., 1944. The essential difference between the two optimum proportions flocculation ratios. J. Exp. Med. 80, 289.

Finney, D.J., 1978. Statistical Methods in Biological Assay, 3rd ed. Charles Griffin, London.

Glenny, A.T., Okell, C.C., 1924. The titration of diphtheria toxin and antitoxin by flocculation methods. J. Pathol. Bacteriol. 27, 187.

Harrison, P., 2000. Progress in the assessment of platelet function. Br. J. Haematol. 111, 733.

Jacobsen, C., Steensgaard, J., 1979. Measurements of precipitin reactions by difference turbidimetry: a new method. Immunology 36, 293.

Künzel, A., Scherkowski, D., Willers, R., Becker, J., 2003. Visually detectable resolution of intraoral dental films. Dento-Maxillo-Facial Radiol. 32, 385.

Levine, L., Wyman, L., 1965. The flocculation test and the law of mass action. J. Immunol. 94, 586.

Lyng, J., Bentzon, M.W., 1987. The quantitative estimation of diphtheria and tetanus toxoids. 1. The flocculation test and the Lf-unit. J. Biol. Stand. 15, 27.

Murata, R., Kubota, K., Kawashima, S., 1953. Studies on the flocculation of tetanus antitoxins by flocculation. Jpn. J. Med. Sci. Biol. 6, 331.

Ozaki, Y., Satoh, K., Yatomi, Y., Yamamoto, T., Shirasawa, Y., Kume, S., 1994. Detection of platelet aggregates with a particle counting method using light scattering. Anal. Biochem. 218, 284.

Ramon, G., 1922a. Floculation dans un mélange neutre de toxine-antitoxine diphthériques. Compt. Rend. Soc. Biol. 86, 661.

Ramon, G., 1922b. A propos du titrage *in vitro* du sérum antidiphthérique par la flocculation. Compt. Rend. Soc. Biol. 86, 813.

Ramon, G., 1922c. Sur une technique de tirage *in vitro* du sérum antidiphthérique. Compt. Rend. Soc. Biol. 86, 711.

WHO Expert Committee on Biological Standardization, 1990. Annex 2, Requirements for diphtheria, tetanus, pertussis and combined vaccines (Requirements for biological substances Nos. 8 and 10). WHO Technical Report Series, vol. 800. World Health Organization, Geneva, p. 87.

World Health Organization, 1977a. Appendix D.7 Determination of Lf/ml. WHO Manual for the Production and Control of Vaccines: Diphtheria Toxoid, BLG/UNDP. World Health Organization, Geneva, p. 60.

World Health Organization, 1977b. Appendix T.5 Determination of Lf/ml. In: WHO (Ed.), Manual for the Production and Control of Vaccines: Tetanus Toxoid, BLG/UNDP. World Health Organization, Geneva, p. 55.

Yamamoto, T., Egawa, Y., Shirasawa, Y., Ozaki, Y., Sato, K., Yatomi, Y., Kume, H., 1995. A laser light scattering *in situ* system for counting aggregates in blood platelet aggregation. Meas. Sci. Technol. 6, 174.

ARTICLE IN PRESS

Available online at www.sciencedirect.com

ScienceDirect

Microbial Pathogenesis ▮ (▮▮▮▮) ▮▮–▮▮

MICROBIAL PATHOGENESIS

www.elsevier.com/locate/micpath

Identification of the receptor-binding sites in the carboxyl-terminal half of the heavy chain of botulinum neurotoxin types C and D

Kentaro Tsukamoto[a], Yuiko Kozai[b], Hideshi Ihara[c], Tomoko Kohda[b], Masafumi Mukamoto[b], Takao Tsuji[a], Shunji Kozaki[b,*]

[a]*Department of Microbiology, Fujita Health University School of Medicine, Toyoake, Aichi 470 1192, Japan*

[b]*Department of Veterinary Science, Graduate School of Life and Environmental Sciences, Osaka Prefecture University, 1-1 Gakuen-cho, Naka-ku, Sakai, Osaka 599 8531, Japan*

[c]*Department of Biological Science, Graduate School of Science, Osaka Prefecture University, 1-1 Gakuen-cho, Naka-ku, Sakai, Osaka 599 8531, Japan*

Received 4 October 2007; received in revised form 11 December 2007; accepted 14 December 2007

Abstract

Botulinum neurotoxin (BoNT) binds to presynaptic neuronal cells and blocks neurotransmitter release. The carboxyl-terminal half of the heavy chain (H_C) of the neurotoxin recognizes its specific receptor on the plasma membrane. We have previously demonstrated that BoNT/C binds to gangliosides GD1b and GT1b under physiological conditions, while BoNT/D interacts with phosphatidylethanolamine (PE). Here we report that the recognition sites for gangliosides and PE are present in the carboxyl-terminal domain of H_C. Chimeric mutants and site-directed mutants of BoNT/C-H_C and BoNT/D-H_C were generated and their binding activities evaluated. The chimeric H_C that consisted of the amino-terminal half of BoNT/D-H_C and the carboxyl-terminal half of BoNT/C-H_C possessed activity similar to the authentic BoNT/C-H_C, suggesting that the carboxyl-terminal region of H_C is involved in the receptor recognition of BoNT/C. Moreover, analysis using site-directed mutants indicated that the peptide motif $W^{1257}Y\cdots G^{1270}\cdots H^{1282}$ plays an important role in the interaction between BoNT/C and gangliosides. In contrast, we revealed that two lysine residues of BoNT/D-H_C are involved in the formation of the critical binding site for receptor binding.

1. Introduction

Seven distinct types of botulinum neurotoxins (BoNTs/A–G) produced by *Clostridium botulinum* are the causative agents of botulism [1]. BoNTs/A, B, E, and F are the most potent in causing human intoxication, and BoNTs/C and D are responsible for avian and animal botulism [2,3]. Some type C strains produce unique BoNT called C/D mosaic toxin (BoNT/CD) that comprises two thirds of BoNT/C and one third of BoNT/D corresponding to the H_C portion [4,5]. These neurotoxins as well as the other clostridial toxin, tetanus neurotoxin (TeNT), are synthesized as a single polypeptide chain molecule with a molecular mass of about 150 kDa, and thereafter nicked by proteases into heavy (100 kDa) and light (50 kDa) chains linked together by a disulfide bond. The light chain is a zinc endopeptidase that cleaves the presynaptic soluble *N*-ethylmaleimide-sensitive factor attachment protein receptor (SNARE) proteins [6–9]. Assembly of SNARE proteins is an essential step in neuroexocytosis. The correlation between SNARE protein cleavage by BoNTs and the blockade of neurotransmission is well documented [10–12]. The heavy chain mediates binding to neuronal receptors, leading to internalization of the light chain and its translocation into the cytoplasm of nerve terminals [13,14].

The specific binding of neurotoxin to the peripheral neuromuscular junction is considered to be the first step in intoxication. It is well known that the adhesion between neurotoxins and nerve endings involves gangliosides [15–18], and the carboxyl-terminal half domain of the heavy chain (H_C) binds to the gangliosides. The domain is

Abbreviations: BoNT, botulinum neurotoxin; H_C, carboxyl-terminal domain of the heavy chain; SNARE, soluble *N*-ethylmaleimide-sensitive factor attachment protein receptor; PE, phosphatidylethanolamine.

*Corresponding author. Tel.: +81 72 254 9504; fax: +81 72 254 9499.
E-mail address: kozaki@center.osakafu-u.ac.jp (S. Kozaki).

0882-4010/$ - see front matter © 2008 Published by Elsevier Ltd.
doi:10.1016/j.micpath.2007.12.003

Please cite this article as: Tsukamoto K, et al. Identification of the receptor-binding sites in the carboxyl-terminal half of the heavy chain of botulinum neurotoxin types C and D. Microb Pathog (2008), doi:10.1016/j.micpath.2007.12.003

composed of two subdomains; an amino-terminal jelly roll (H_{CN}) and a carboxyl-terminal β-trefoil (H_{CC}). The crystallographic data on BoNTs/A and B revealed that H_{CC} subdomains structurally resemble the lactose-binding pocket of TeNT [19–23], but the H_{CC} amino acid sequence is poorly conserved among BoNTs. Hence, BoNTs are considered to recognize type-specific receptors other than gangliosides. Synaptotagmin I and II, two homologous synaptic vesicle proteins, have been indicated to function in the entry of BoNT/B into neuronal cells [24–26]. Meanwhile, Synaptic vesicle protein SV2 acts as the protein receptor for BoNT/A [27,28]. We previously reported that the receptor for BoNTs/C and D might not include a protein component, as opposed to BoNTs A and B. In BoNT/C, unlike other types of BoNTs, gangliosides are predicted to play a significant role in the binding to neuronal cells, because a deficiency of gangliosides produced little sensitivity to BoNT/C *in vivo* [29]. On the other hand, BoNT/D exhibited binding activity to phosphatidylethanolamine (PE). These findings suggest that the binding sites in BoNTs/C and D molecules are possibly maintained in different amino acid residues compared with TeNT and BoNTs/A and B. To clarify this diversity, the present study is an attempt to identify the crucial region in BoNTs/C and D for binding to the receptor by using chimeric and site-directed H_C mutants.

2. Materials and methods

2.1. Preparation of recombinant H_C

Wild-type and mutant H_C proteins (type C: H_C/C, type D: H_C/D_1 and H_C/D_2) were expressed and purified as described previously [29]. H_C/C was originated from

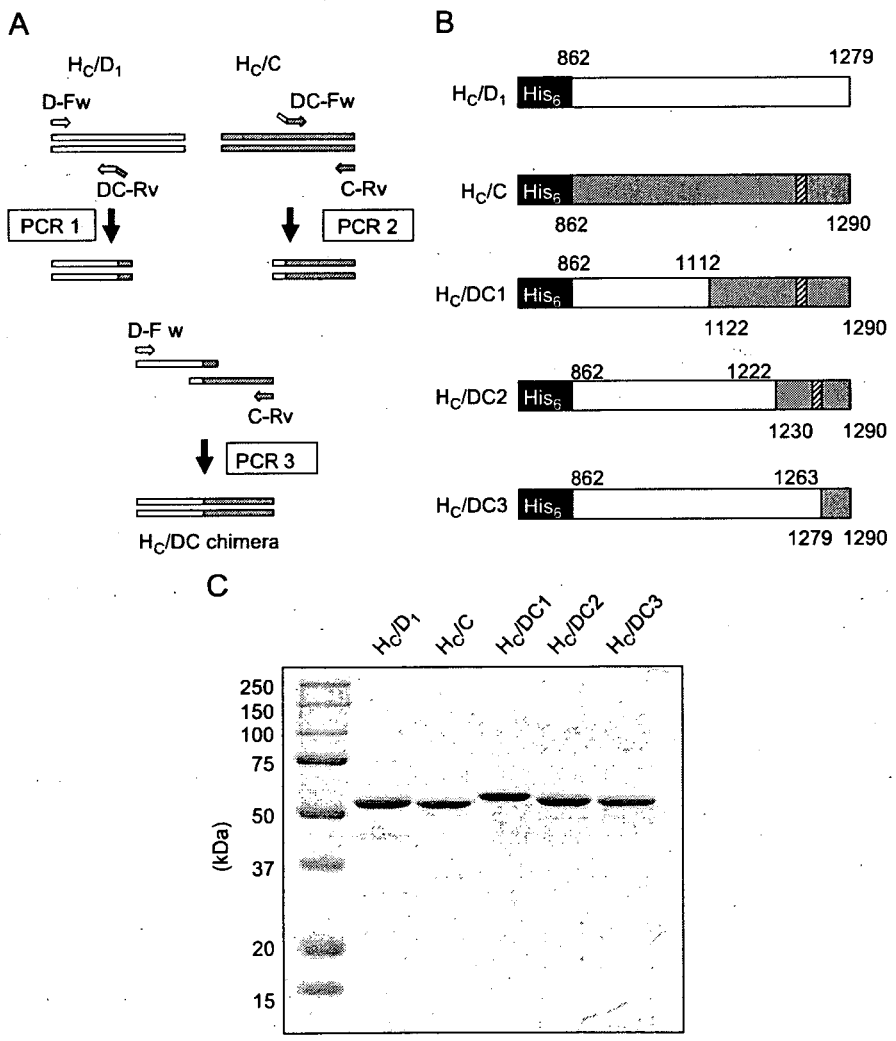

Fig. 1. Preparation of chimeric H_C mutants: (A) schematic overview of overlap extension PCR. Two separate DNA fragments were amplified in PCR reactions 1 and 2. The primers DC-Rv and DC-Fw introduce overlapping regions. These overlap regions hybridize in PCR reaction 3. Thus, using the primers D-Fw and C-Rv the full-length chimeric H_C fragment was finally amplified; (B) schematic representation of the recombinant wild-type H_C and the chimeric H_C. The squares filled by oblique lines indicate the ganglioside-binding motif. The numbers correspond to the position of the amino acids; and (C) SDS-PAGE profile of the recombinant H_C. The sample (1 μg/lane) was applied to a 10% polyacrylamide gel.

Please cite this article as: Tsukamoto K, et al. Identification of the receptor-binding sites in the carboxyl-terminal half of the heavy chain of botulinum neurotoxin types C and D. Microb Pathog (2008), doi:10.1016/j.micpath.2007.12.003

typical type C toxin (strain CB-19). H_C/D_1 was derived from BoNT/CD (strain 003-9). H_C/D_2 was derived from typical type D toxin (strain 1873). H_C/D_1 showed a binding activity higher than H_C/D_2 [29]. Overlap extension PCR for the construction of genes encoding chimeric polypeptides was carried out as described originally [30]. In two separate PCR amplifications (the products of PCR 1 and 2), double-stranded fragments were generated and subsequently fused in PCR 3 (Fig. 1A). PCR 1 used a common 5′-far primer (D-Fw) and the unique reverse overlap primer (DC-Rv) that carries information for the construction of the intended chimera (Table 1). In PCR 2, a 3′-far primer (C-Rv) from the stop codon of the BoNT/C gene and a primer that was the complement of the overlap primer used in PCR 1 (DC-Fw) were used to generate the carboxyl-terminal fragment. After the two PCR products were mixed, denatured, and cooled, the complementary overlaps annealed, and the junction was then extended by template-dependent DNA polymeryzation. Finally, the chimeric construct was amplified by using far primers (D-Fw and C-Rv), and the amplified fragment was cloned into vector pET-30a (Novagen, Darmstadt, Germany). H_C/DC1 was composed of the amino acid residues 862-1112 of BoNT/CD and 1122–1290 of BoNT/C. H_C/DC2 comprised the residues 862-1222 of BoNT/CD and residues 1230–1290 of BoNT/C. The two chimeric mutants contain the ganglioside-binding motif (Fig. 1B). H_C/DC3 consisted of residues 862–1263 of BoNT/CD and residues 1279–1290 of BoNT/C. H_C/DC3 possessed the G1270-containing ganglioside-binding motif, but not motifs W1257 and Y1258. The chimeric mutants that consisted of H_C/D_1 and H_C/D_2 (H_C/DD1-H_C/DD4) were constructed using suitable primers in a similar manner (Fig. 2A). These chimeric H_Cs were composed of C-terminal H_C/D_1 (high affinity binding) and N-terminal H_C/D_2 (low affinity binding). Site-directed mutations were introduced into the H_C/C, H_C/D_1, and H_C/D_2 genes in pET-30a by using a QuickChange site-directed mutagenesis kit (Stratagene, La Jolla, CA) as instructed by the manufacturer. Briefly, suitable primers were designed for the desired mutation, and a thermocycling reaction permitted *in vitro* synthesis of the plasmid DNA with *PfuUltra*™ high-fidelity DNA polymerase (Stratagene). Parental methylated template DNA was digested by DpnI, and the resultant mutated plasmid mixture was used to transform *Escherichia coli* JM109 cells. All mutants were sequenced and expressed in *E. coli* BL21 CodonPlus (DE3)-RIL (Stratagene) in a similar manner to the wild-type H_C.

2.2. Binding of H_C to synaptosomes

Wild-type recombinant H_C proteins were radioiodinated with $Na^{125}I$ (Perkin Elmer Japan, Yokohama, Japan) using the chloramine-T method as described previously [31]. The specific activities of the H_C proteins ranged from 13 to 17 mCi/mg protein (26–34 MBq/nmol). Synaptosomes were prepared from rat brain [32] and suspended in *N*-2-hydroxyethylpiperazine-*N*′-2-ethanesulfonic acid (HEPES) buffered saline (HBS) [3 mM HEPES–NaOH buffer (pH 7.0) containing 150 mM NaCl, 2.5 mM KCl, 2 mM $MgCl_2$, and 2 mM $CaCl_2$]. The binding of ^{125}I-H_C to the synaptosomes was measured by a filtration assay in the presence or absence of unlabeled H_C or cinnamycin (Ro 09-198) (Sigma, Tokyo, Japan) [33].

Table 1
Specific primers used for preparation of chimera H_C by overlap extension PCR

Primer	Sequence[b]
D-Fw	5′-CATGCCATGGCTGAATATTTCAATAGTATTAATGATTCA-3′[c]
C-Rv[a]	5′-CCCAAGCTTTTATTCACTTACAGGTACAAAACC-3′[d]
D-Rv	5′-CCCAAGCTTTTACTCTACCCATCCTGGATC-3′[d]
DC1-Fw	5′-TAATTATAATTATATAGATAGG/TATATGTATGCGAACTCACG-3′
DC1-Rv[a]	5′-CGTGAGTTCGCATACATATA/CCTATCTATATAATTATAATTA-3′
DC2-Fw	5′-GTATCTCAAAATAAATATTGTAGTCAA/ATATTTAAATCAAATTTTAATGGAGAAA-3′
DC2-Rv[a]	5′-TTTCTCCATTAAAATTTGATTTAAATAT/TTGACTACAATATTTATTTTGAGATAC-3′
DC3-Fw	5′-CTAATTATGAGACAAAACTATTATCA/ACATCAACTCATTGGGGTT-3′
DC3-Rv[a]	5′-AACCCCAATGAGTTGATGT/TGATAATAGTTTTGTCTCATAATTAG-3′
DD1-Fw	5′-ATGGAGATAATATAATTCTTCAT/TCTAAAGATTTAACTAATTCTCATA-3′
DD1-Rv[a]	5′-TATGAGAATTAGTTAAATCTTTAGA/ATGAAGAATTATATTATCTCCAT-3′
DD2-Fw	5′-GATCTAAATTATATACTGGAAATCCTATT/ACTATTAAATCAGCAGCTAATAAGA-3′
DD2-Rv[a]	5′-TCTTATTAGCTGCTGATTTAATAGT/AATAGGATTTCCAGTATATAATTTAGATC-3′
DD3-Fw	5′-GATACAGAATATTATATTATTAATGATAATTATATAGAT/AGGTATATAGCACCTAAAAATAATATACT-3′
DD3-Rv[a]	5′-AGTATATTATTTTTAGGTGCTATATACCT/ATCTATATAATTATCATTAATAATATAATATTCTGTATC-3′
DD4-Fw	5′-TAGTGTTAGTTTTTGGATTAAGATA/TCTAAAGATTTAACTAATTCTCATA-3′
DD4-Rv[a]	5′-TATGAGAATTAGTTAAATCTTTAGA/TATCTTAATCCAAAAACTAACACTA-3′

[a]Oligonucleotide positioned in the complementary strand.
[b]Slashes in parentheses indicate the position of overlap junctions.
[c]The underline indicates Nco I site.
[d]The underline indicates Hind III site.

Please cite this article as: Tsukamoto K, et al. Identification of the receptor-binding sites in the carboxyl-terminal half of the heavy chain of botulinum neurotoxin types C and D. Microb Pathog (2008), doi:10.1016/j.micpath.2007.12.003

2.3. TLC overlay assay

The recombinant H_C proteins were biotinylated with EZ-Link™ Sulfo-NHS-LC-biotin (Pierce, Rockford, IL). The gangliosides GD1b and GT1b (Sigma) (0.25 nmol each) and PE from bovine brain (Sigma) (0.5 nmol) were chromatographed on plastic-coated TLC plates (Macherey-Nagel, Düren, Germany) in chloroform/methanol/water 5:4:1 (v/v). The TLC plates were then dried and blocked with Blocking One (Nacalai Tesque, Kyoto, Japan) containing 1% polyvinylpyrrolidone for 12 h at 4 °C. After blocking, the plates were incubated with 5 nM biotinylated H_C for 2 h at 37 °C in HBS. After washing three times in HBS to remove unbound H_C, the plates were incubated with 1 μg/ml horseradish peroxidase (HRP)-conjugated avidin (Zymed Laboratories Inc., San Francisco, CA). The H_C binding lipids were detected using 3,3′-diamino-benzidine (DAB)-stable substrate solution (Wako, Osaka, Japan).

2.4. Others

Sodium dodecyl sulfate-polyacrylamide gel electrophoresis (SDS-PAGE) was performed using 10% gels by the method used by Laemmli [34]. Protein concentration was determined by Lowry's method using bovine serum albumin as a standard [35].

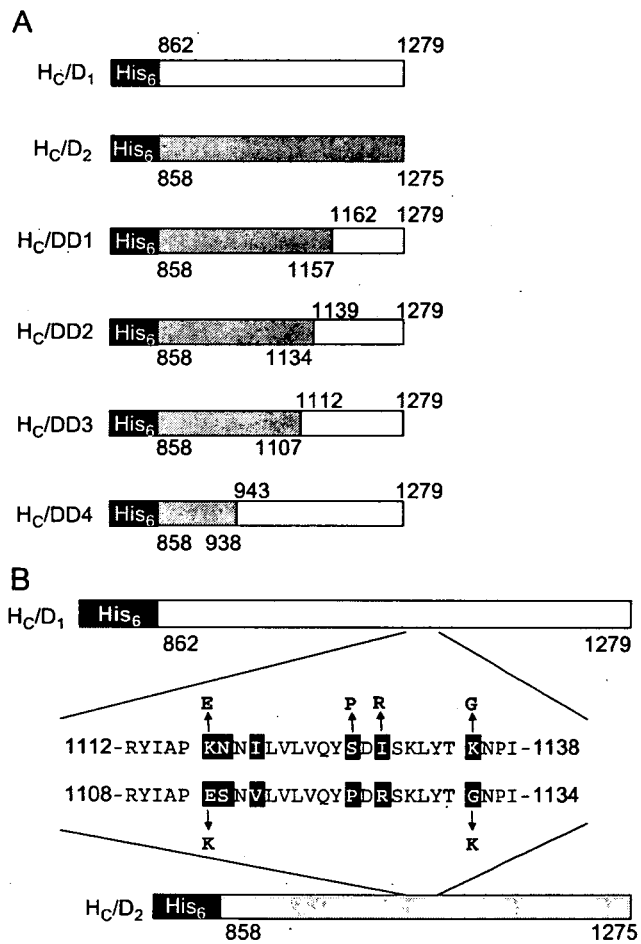

Fig. 2. Preparation of chimeric mutants and site-directed mutants of H_C/D: (A) schematic representation of the recombinant wild-type H_C and chimeric H_C. The numbers correspond to the position of the amino acids and (B) schematic representation of the recombinant site-directed mutants and the amino acid sequence of the region targeted for mutagenesis in this study.

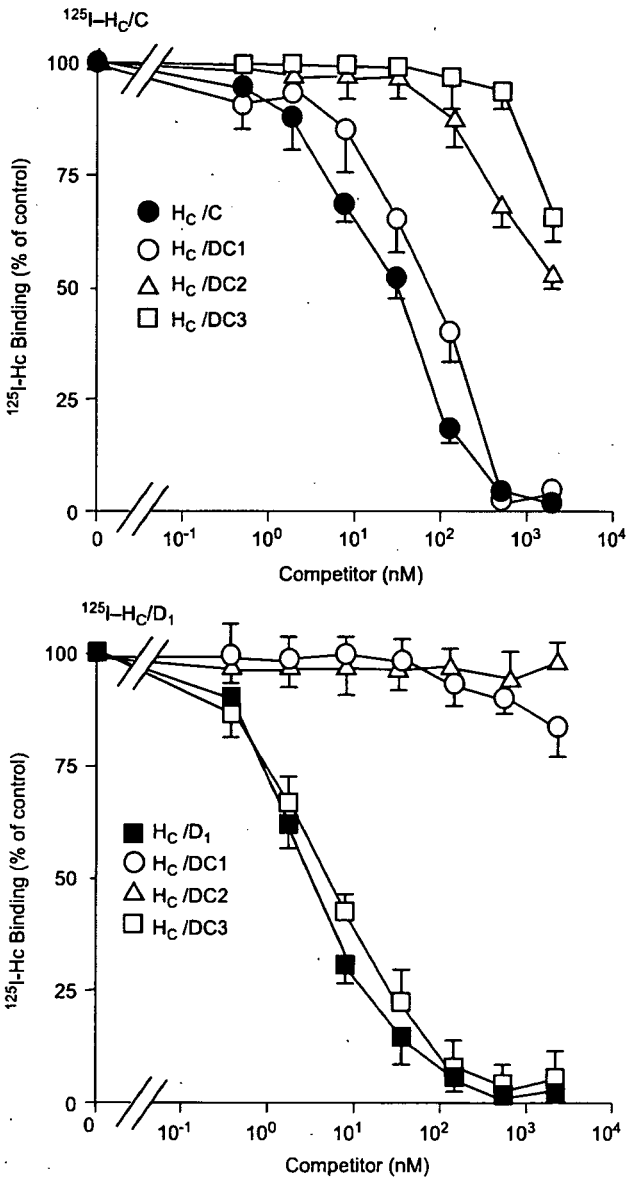

Fig. 3. Competition binding assay of ^{125}I-H_C/C and H_C/D_1 to rat brain synaptosomes with wild type and D/C chimeric H_C. ^{125}I-H_C (0.5 nM) was incubated with synaptosomes (1 μg protein in 0.2 ml) at 37 °C for 60 min in the presence of various concentrations of unlabeled H_C. Each data point represents the mean±S.D. from three separate experiments each performed in duplicate.

Please cite this article as: Tsukamoto K, et al. Identification of the receptor-binding sites in the carboxyl-terminal half of the heavy chain of botulinum neurotoxin types C and D. Microb Pathog (2008), doi:10.1016/j.micpath.2007.12.003

3. Results

3.1. Expression and binding activities of DC chimeric H_c

We previously constructed H_C genes (H_C/C, H_C/D_1, and H_C/D_2) in pET-30a and obtained recombinant proteins that possessed binding activities similar to that of the neurotoxins [29].

To examine the recognition site for the receptor, we generated three kinds of chimeric H_C (H_C/DC1, H_C/DC2, and H_C/DC3) using overlap extension PCR (Fig. 1B). SDS-PAGE profiles revealed that all recombinant proteins were successfully obtained in a pure state (Fig. 1C).

To evaluate the binding activity of the chimeric H_C, we performed a binding experiment using ^{125}I-wild-type H_C (Fig. 3). H_C/DC1 effectively inhibited the binding of ^{125}I-H_C/C to synaptosomes but not that of ^{125}I-H_C/D_1, whereas H_C/DC3 exhibited an inhibitory effect on the binding of ^{125}I-H_C/D_1. H_C/DC2 did not show any inhibitory effect on the binding of either ^{125}I-H_C/D_1 or ^{125}I-H_C/C. In order to characterize the binding specificity of chimeric H_C, a TLC overlay assay was performed (Fig. 4). H_C/DC1 was found to bind GD1b and GT1b, but not PE. On the other hand, H_C/DC3 retained the PE binding ability. H_C/DC2 hardly associated with any lipid molecules.

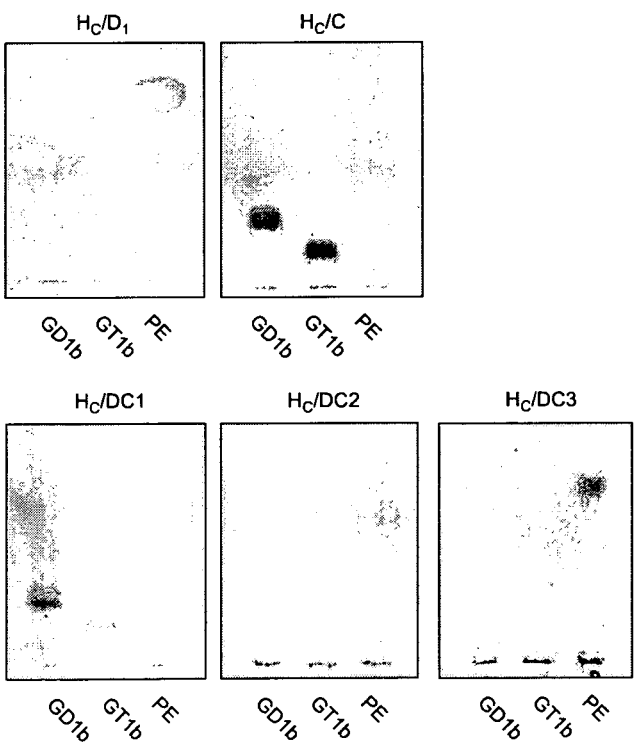

Fig. 4. TLC overlay analysis to detect the direct binding of H_C to lipid receptors. Gangliosides (0.25 nmol) and phosphatidylethanolamine (1 nmol) were chromatographed on plastic-coated TLC plates. After blocking, the plates were incubated with 5 nM biotinylated H_C at 37 °C for 2 h in HBS, followed by treatment with 1 μg/ml HRP-avidin. The H_C binding lipids were detected using DAB substrate solution.

3.2. Determination of the critical amino acid residues involved in ganglioside-binding

Since previous chimeric mutagenesis studies had implicated the region between Y1122 and S1278 of BoNT/C as being important for ganglioside-binding, eight single point mutations of H_C/C were generated using the QuickChange kit. All mutations were confirmed by nucleotide sequencing of both strands of the mutated H_C/C. The previous experiments with TeNT found that the lactose binding site is characterized by the presence of the peptide motif H···SXWY···G [36]. The motif is conserved among most BoNTs (Fig. 5). Especially, W1283 in BoNT/C is common residues among all clostridial neurotoxins, but residue H1282, which has a positive charge, specifically exists immediately prior to W1283 in only BoNT/C. We thus constructed mutants with single amino acid changes in H_C/C, as the following W1257A, W1257F, Y1258A, G1270A, H1282A, H1282E, W1283A, and W1283F (Fig. 6), and determined their binding activities with rat brain synaptosomes. All the mutants except for W1283A and W1283F had strong decreases in binding activity against synaptosomes (Fig. 7).

3.3. Binding activity of H_c/D mutants

We showed that H_C/D interacts with PE in the TLC overlay assay, but it was still unclear whether H_C/D could bind to PE on synaptosomes. Cinnamycin (Ro 09-0198), which is a tetracyclic peptide antibiotic, is known to associate with PE [37,38]. To investigate which molecule was recognized by H_C/D on the membrane, the inhibitory effects of cinnamycin on the binding of ^{125}I-H_C/D to rat brain synaptosomes were examined. The binding of H_C/D_1 and H_C/D_2 was inhibited in the presence of cinnamycin in a dose dependent manner, but the binding of H_C/C was not inhibited (Fig. 8).

To explore the critical region for the binding of H_C/D, four kinds of chimeric H_C (H_C/DD1, H_C/DD2, H_C/DD3, and H_C/DD4) were prepared (Fig. 2A). The binding of ^{125}I-labeled H_C/D_1 was competed by unlabeled wild-type H_C/D_1 and H_C/D_2 in a concentration dependent manner, whose IC_{50} (50% inhibition concentration) values were 0.4 and 152 nM, respectively (Table 2). H_C/DD1 and H_C/DD2 inhibited the binding of ^{125}I-labeled H_C at the same level as H_C/D_2 (IC_{50} = 178 and 165 nM, respectively), whereas H_C/DD3 and H_C/DD4 were found to possess high affinity binding activity (IC_{50} = 0.7 and 0.4 nM, respectively), whose values were equivalent to that of H_C/D_1. Accordingly, residues 1112–1139 of BoNT/CD are assumed to take part in the formation of the high affinity binding site. In this region, there are six amino acid residue differences between H_C/D_1 and H_C/D_2. To identify the critical residues that participate in the binding, point mutations of H_C/D_1

Please cite this article as: Tsukamoto K, et al. Identification of the receptor-binding sites in the carboxyl-terminal half of the heavy chain of botulinum neurotoxin types C and D. Microb Pathog (2008), doi:10.1016/j.micpath.2007.12.003

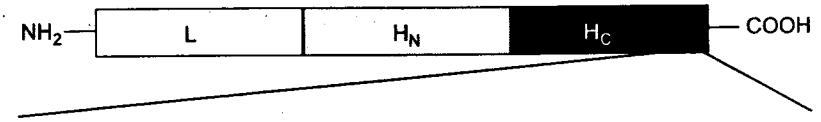


```
A     1221 VMKSKNDQGITNKCKMNL-QDNNGNDIGFIGFHQFNN---------I 1257
B     1209 IKEYDEQP-TYSCQLLFKKDEESTDEIGLIGIHRFYE-SGIVFEEYK 1253
C     1217 IFQIQPMNNTYYYASQIFKSNFNGENISGICSIGTY---------- 1249
D/C   1207 SFIIQPCNTFDYYASQLFLSSNATTNRLGILSIGSYS---------- 1243
C/D   1208 -FSIKNIVSQNKYCSQIF-SSFMKNTMLLADIYKPW---------- 1241
D     1204 -FSIKNIVSKNKYCSQIF-SSFRENTMLLADIYKPW---------- 1237
E     1188 VMNS-----VGNNCTMNF-KNNNGNNIGLLGFKA---------- 1215
F     1214 VMDS-----IGNNCTMNF-QNNNGGNIGLLGFHS---------- 1241
G     1217 KKYYEKT--TYNCQILCEKD---TKTFGLFGIGKFVKDYGYVWDTYD 1259
TeNT  1241 AVKLRDLK--TYSVQLKLY-DDKNASLGLVGTH---NGQIGNDPNR 1280

A     1258 AKLVASNWYNRQIERSSRTL--GCSWEFIPVDD-GWGERPL      1295
B     1254 DYFCISKWYLKEVKRKPYNLKLGCNWQFIPKDE-GWTE        1290
C     1250 RFRLGGDWYRHNYLVPTVKQ--GNYASLLESTSTHWGFVPVSE   1290
D/C   1244 FKLGDDYWFNHEYLIPVIKI--EHYASLLESTSTHWVFVPASE   1284
C/D   1242 RFSFENAY------TPVAVTN--YETKLL-STSSFWKFISRDPGWVE 1279
D     1238 RFSFKNAY------TPVAVTN--YETKLL-STSSFWKFISRDPGWVE 1275
E     1216 DTVVASIWYYTHMRDH--TNSNGCFWNFI-SEEHGWQEK       1251
F     1242 NNLVASSWYYNNIRKN--TSSNGCFWSFI-SKEHGWQEN       1277
G     1260 NYFCISQWYLRRISENINNLRLGCNWQFIPVDE-GWTE        1296
TeNT  1281 DILIASNWYFNHL----KDKILGCDWYFVPTDE-GWTND       1314
                  **          *         **
```

Fig. 5. Amino acid sequence alignment of the carboxyl-terminal region of TeNT and BoNT (A-G). The amino acid residues forming the ganglioside-binding pocket in TeNT and BoNTs/A and B are presented as white letters on a black background. Positions of amino acids of BoNT/C selected for mutational analyses are highlighted by asterisks below the sequence of TeNT.

and H_C/D_2 were generated (Fig. 2B). Consequently, S1127P and I1129R retained the inhibitory effect on the binding of ^{125}I-H_C/D_1 to synaptosomes ($IC_{50} = 0.5$ and 0.3 nM, respectively), but K1117E and K1135G were shown to reduce the binding affinity ($IC_{50} = 173$ and 1.2 nM, respectively) (Table 2). These results indicate that two lysine residues are involved in the binding, but the K1117 is more effective residue than K1135. On the contrary, the mutations E1113K and G1131K in H_C/D_2 were shown to increase the binding affinity ($IC_{50} = 9.1$ and 2.0 nM, respectively). The double mutation of E1113K and G1131K was characteristic of the high affinity binding of authentic H_C/D_1 ($IC_{50} = 0.6$ nM).

4. Discussion

Clostridial neurotoxins bind to nerve terminals through the H_C region derived from the heavy chain. The binding sites on TeNT were localized by co-crystallization experiments and biochemical approaches using TeNT mutants [19,20,36]. The lactose binding site is characterized by the presence of a peptide motif H···SXWY···G. A similar motif is conserved among the BoNTs/A, B, E, F, and G proteins, but not BoNTs/C and D. BoNT/C retains a part of the motif, "WY···G"; however, BoNT/D lacks this peptide motif completely [39]. These observations also suggest that BoNTs/C and D share different properties with respect to the interaction with carbohydrate molecules in comparison with other clostridial toxins. To confirm this hypothesis, we have analyzed the binding properties of H_C mutants at the carboxyl-terminal region of BoNTs/C and D. Our present mutagenesis study has now identified several specific amino acid residues that possess a critical role in binding to gangliosides and PE.

First, we focused on the H_{CC}-subdomain and generated chimeric mutants that comprise parts of BoNT/D-H_C and BoNT/C-H_C by overlap extension PCR. The degree of sequence homology between the BoNT/C-H_C and BoNT/D-H_C genes is 64%, and they have very few restriction sites in common that can be used in constructing chimeric mutants. Therefore, overlap extension PCR was useful to construct the chimeric mutants and to analyze the binding region in BoNT. In the binding experiment using brain synaptosomes, a chimeric H_C that included the carboxyl-terminal half of BoNT/C-H_C (H_C/DC1) exhibited the same level of activity as BoNT/C-H_C, while the other chimeric H_C consisting mainly of BoNT/D-H_C and 11 residues of the carboxyl-terminal of BoNT/C-H_C (H_C/DC3) showed a binding activity similar to that of BoNT/D-H_C. Halpern et al. reported that the removal of H_{CN} from the heavy chain of tetanus neurotoxin did not reduce the binding activity, whereas deletion of only 10 residues from the carboxyl-terminal abolished its binding to spinal cord neurons [40]. However, the present data on

Please cite this article as: Tsukamoto K, et al. Identification of the receptor-binding sites in the carboxyl-terminal half of the heavy chain of botulinum neurotoxin types C and D. Microb Pathog (2008), doi:10.1016/j.micpath.2007.12.003

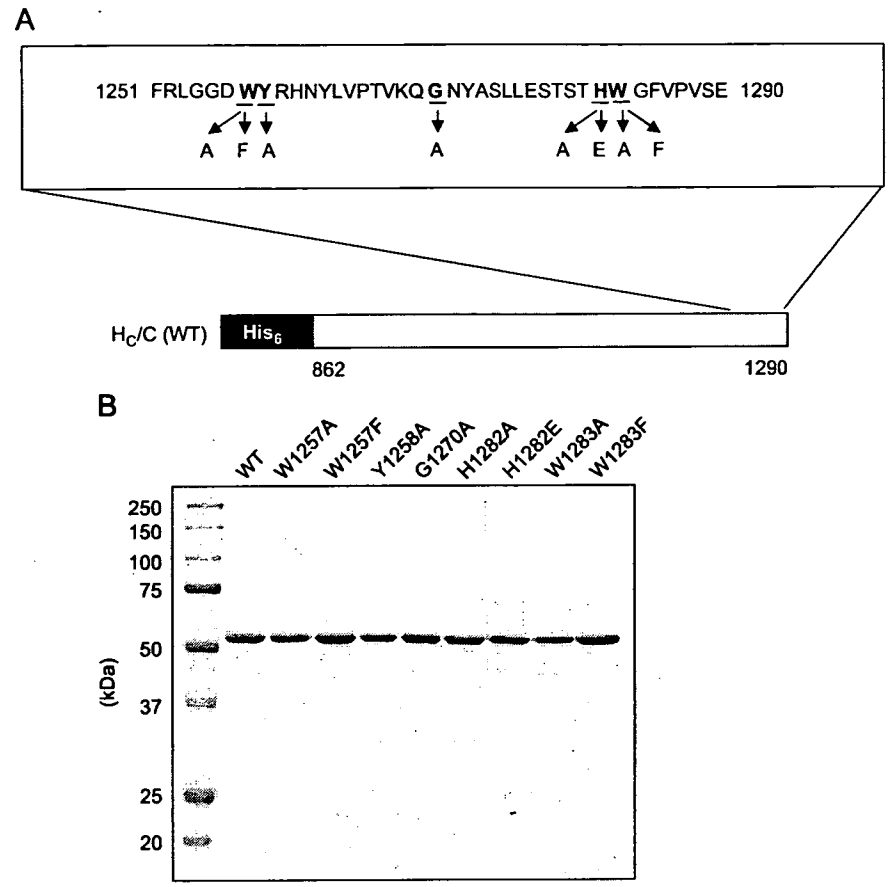

Fig. 6. Preparation of site-directed mutants of H_C/C: (A) schematic representation of the recombinant site-directed mutants and the amino acid sequence of the region targeted for mutagenesis in this study and (B) SDS-PAGE profile of the recombinant H_C. The sample (1 μg/lane) was applied to a 10% polyacrylamide gel.

BoNT/D showed that the carboxyl-terminus 10 residues of BoNT/D were not involved in the binding because H_C/DC3 retained its ability to bind to PE. H_C/DC1 actually bound both gangliosides GD1b and GT1b but not PE, whereas H_C/DC3 interacted only with PE. Although H_C/DC2 contained ganglioside-binding motif, H_C/DC2 was not able to recognize any molecule. This discrepancy is not able to explain clearly. The binding region of H_C/DC2 was probably hooded, owing to the conformational change by chimeric mutation. These results suggest that the binding site for PE formed an inherent structure. Consequently, this study documents the critical regions of the H_{CC}-subdomain of BoNT/C in receptor recognition. In BoNT/C, the recognition site for GD1b and GT1b is located within amino acid residues 1122–1290. In BoNT/D, these results show a loss of inhibition of H_C/DC1 and H_C/DC2 on ^{125}I-H_C/D_1 binding, thus suggesting, according to Fig. 1B, a recognition site located within amino acid residues 1222–1279. Even more, this site can be restricted to 1222–1263, as amino acid residues 1264–1279 of BoNT/CD do not appear to be necessary for the inhibition to occur as they can be replaced by amino acid residues 1279–1290 of BoNT/C.

Second, we have generated eight single point mutants of five amino acid residues to clarify the molecular interactions between the BoNT/C H_C residues of the deduced binding site and gangliosides. In BoNT/C molecules, a part of the ganglioside binding pocket (WY···G), which are conserved in TeNT, BoNT/A, and BoNT/B, is observed. We have carried out substitutions of W1257, Y1258, G1270, H1282, and W1283. H1282 is the amino acid residue that possesses a positive charge and exists only in BoNT/C. W1283 is a common residue conserved in all clostridial neurotoxins. Mutations of W1257, Y1258, and G1270, residues located in positions comparable to the ganglioside-binding pockets of TeNT and BoNTs/A and B, dramatically affected the binding activity. Since the decrease in binding activity was observed in not only W1257A but also W1257F, the indole ring of W1257 is thought to be essential, forming strong interactions with the hydrophobic side of the sugar ring. This finding suggests that W1257, Y1258, and G1270 form a ganglioside-binding pocket in BoNT/C as well as other types of neurotoxins. The influence of the histidine on the functionality of the BoNT/C binding pocket is also important. The glutamate substitution of H1282 is more

Please cite this article as: Tsukamoto K, et al. Identification of the receptor-binding sites in the carboxyl-terminal half of the heavy chain of botulinum neurotoxin types C and D. Microb Pathog (2008), doi:10.1016/j.micpath.2007.12.003

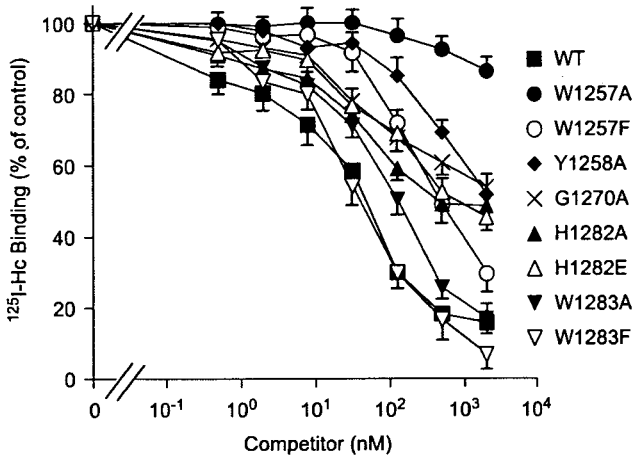

H_C	IC_{50} (nM)
WT	21
W1257A	>1000
W1257F	297
Y1258A	>1000
G1270A	448
H1282A	151
H1282E	267
W1283A	56
W1283F	14

Fig. 7. Competition binding assay of ^{125}I-H_C/C to rat brain synaptosomes with site-directed mutants of H_C/C. ^{125}I-H_C/C (0.5 nM) was incubated with synaptosomes (1 μg protein in 0.2 ml) at 37°C for 60 min in the presence of various concentrations of unlabeled H_C. Each data point represents the mean±S.D. from three separate experiments each performed in duplicate.

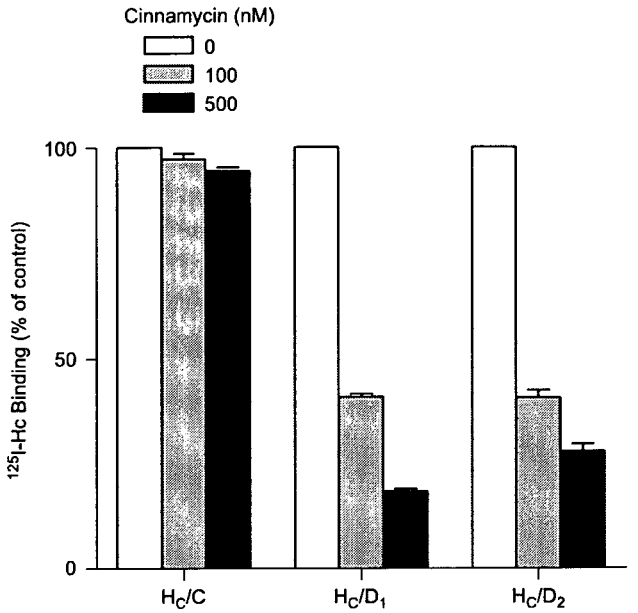

Fig. 8. Effect of cinnamycin on the binding of ^{125}I-H_C to rat brain synaptosomes. ^{125}I-H_C (0.5 nM) was incubated with synaptosomes (1 μg protein in 0.2 ml) at 37°C for 60 min in the presence of various concentrations (0, 100, and 500 nM) of cinnamycin. Each data point represents the mean±S.D. from three separate experiments each performed in duplicate.

Table 2
Binding activity of H_C/D mutants

Recombinant H_C	Binding activity[a] (nM)
Wild type	
D_1	0.4
D_2	152
Chimeric mutant	
DD1	178
DD2	165
DD3	0.7
DD4	0.4
Site-directed mutant of H_C/D_1	
K1117E	173
S1127P	0.5
I1129R	0.3
K1135G	1.2
Site-directed mutant of H_C/D_2	
E1113K	9.1
G1131K	2.0
E1113K/G1131K	0.6

[a]Data are the concentrations for 50% binding inhibition by competition binding assays of ^{125}I-labeled H_C/D_1.

effective than the alanine substitution, indicating that the positive charge of H1282 of BoNT/C enhances the binding affinity to gangliosides. Unlike other neurotoxins, BoNT/C is able to bind to gangliosides under physiological ionic strength (0.15 M NaCl) [29]. H1282 is most probably a key amino acid in the high affinity binding of BoNT/C to gangliosides. On the other hand, the mutation of W1283 barely affected the binding, suggesting that W1283 of BoNT/C is not including in the ganglioside-binding pocket.

Third, we focused on the binding site of PE in BoNT/D-H_C. Cinnamycin (Ro 09-0198), which binds specifically to PE [37,38], was used as a competitor of BoNT/D-H_C binding to brain synaptosomes. Interaction of BoNT/D-H_C but not BoNT/C-H_C with synaptosomes was inhibited by the presence of cinnamycin, supporting the notion that BoNT/D-H_C recognized PE on the membranes of brain synaptosomes. For the purpose of identification of the binding region of BoNT/D, we examined the binding activity of four chimeric mutants (H_C/DD1–H_C/DD4) and seven site-directed mutants. As a result, two lysine residues (K1117 and K1135 in H_C/D_1) were the most important amino acid residues in the high affinity binding of BoNT/D to PE. Unlike other types, the C-terminal region of H_C is not probably involved in the recognition of its receptor.

Recently, it was reported that TeNT possesses two binding sites against carbohydrate causing higher affinity to gangliosides than BoNTs/A and B [36,39]. Whether

Please cite this article as: Tsukamoto K, et al. Identification of the receptor-binding sites in the carboxyl-terminal half of the heavy chain of botulinum neurotoxin types C and D. Microb Pathog (2008), doi:10.1016/j.micpath.2007.12.003

BoNT/C contains multiple binding sites is not clear, though the high affinity binding of BoNT/C to gangliosides indicates this possibility. Accordingly, the crystallographic analysis provides useful information to clarify the interaction between BoNT/C and gangliosides. In conclusion, these findings are valuable in that we have elucidated the role of BoNTs/C and D. Although additional studies using other mutants of BoNT/C-H_C and BoNT/D-H_C and three dimensional structural analyses are needed to clarify the form of the binding regions, the present study will be useful in developing effective binding inhibitors or therapeutic agents against neuronal disorders.

Acknowledgments

This work was supported in part by Grants-in-Aid for Scientific Research from the Japan Society for the Promotion of Science and from the Ministry of Education, Culture, Sports, Science and Technology of Japan.

References

[1] Simpson LL. Molecular pharmacology of botulinum toxin and tetanus toxin. Annu Rev Pharmacol Toxicol 1986;26:427–53.
[2] Collins MD, East AK. Phylogeny and taxonomy of the food-borne pathogen *Clostridium botulinum* and its neurotoxins. J Appl Microbiol 1998;84:5–17.
[3] Takeda M, Tsukamoto K, Kohda T, Matsui M, Mukamoto M, Kozaki S. Characterization of the neurotoxin produced by isolates associated with avian botulism. Avian Dis 2005;49:376–81.
[4] Moriishi K, Koura M, Abe N, Fujii N, Fujinaga Y, Inoue K, et al. Mosaic structures of neurotoxins produced from *Clostridium botulinum* types C and D organisms. Biochim Biophys Acta 1996; 1307:123–6.
[5] Moriishi K, Koura M, Fujii N, Fujinaga Y, Inoue K, Syuto B, et al. Molecular cloning of the gene encoding the mosaic neurotoxin, composed of parts of botulinum neurotoxin types C1 and D, and PCR detection of this gene from *Clostridium botulinum* type C organisms. Appl Environ Microbiol 1996;62:662–7.
[6] Blasi J, Chapman ER, Yamasaki S, Binz T, Niemann H, Jahn R. Botulinum neurotoxin C1 blocks neurotransmitter release by means of cleaving HPC-1/syntaxin. EMBO J 1993;12:4821–8.
[7] Montecucco C, Schiavo G. Mechanism of action of tetanus and botulinum neurotoxins. Mol Microbiol 1994;13:1–8.
[8] Niemann H, Blasi J, Jahn R. Clostridial neurotoxins: new tools for dissecting exocytosis. Trends Cell Biol 1994;4:179–85.
[9] Yamasaki S, Baumeister A, Binz T, Blasi J, Link E, Cornille F, et al. Cleavage of members of the synaptobrevin/VAMP family by types D and F botulinal neurotoxins and tetanus toxin. J Biol Chem 1994; 269:12764–72.
[10] Breidenbach MA, Brunger AT. New insights into clostridial neurotoxin—SNARE interactions. Trends Mol Med 2005;11:377–81.
[11] Fu Z, Chen S, Baldwin MR, Boldt GE, Crawford A, Janda KD, et al. Light chain of botulinum neurotoxin serotype A: structural resolution of a catalytic intermediate. Biochemistry 2006;45:8903–11.
[12] Schiavo G, Matteoli M, Montecucco C. Neurotoxins affecting neuroexocytosis. Physiol Rev 2000;80:717–66.
[13] Blaustein RO, Germann WJ, Finkelstein A, DasGupta BR. The N-terminal half of the heavy chain of botulinum type A neurotoxin forms channels in planar phospholipid bilayers. FEBS Lett 1987;226:115–20.
[14] Lebeda FJ, Olson MA. Structural predictions of the channel-forming region of botulinum neurotoxin heavy chain. Toxicon 1995;33: 559–67.
[15] Kamata Y, Kozaki S, Sakaguchi G, Iwamori M, Nagai Y. Evidence for direct binding of *Clostridium botulinum* type E derivative toxin and its fragments to gangliosides and free fatty acids. Biochem Biophys Res Commun 1986;140:1015–9.
[16] Takamizawa K, Iwamori M, Kozaki S, Sakaguchi G, Tanaka R, Takayama H, et al. TLC immunostaining characterization of *Clostridium botulinum* type A neurotoxin binding to gangliosides and free fatty acids. FEBS Lett 1986;201:229–32.
[17] Van Heyningen WE, Miller PA. The fixation of tetanus toxin by ganglioside. J Gen Microbiol 1961;24:107–19.
[18] Yowler BC, Kensinger RD, Schengrund CL. Botulinum neurotoxin A activity is dependent upon the presence of specific gangliosides in neuroblastoma cells expressing synaptotagmin I. J Biol Chem 2002;277:32815–9.
[19] Emsley P, Fotinou C, Black I, Fairweather NF, Charles IG, Watts C, et al. The structures of the H_C fragment of tetanus toxin with carbohydrate subunit complexes provide insight into ganglioside binding. J Biol Chem 2000;275:8889–94.
[20] Fotinou C, Emsley P, Black I, Ando H, Ishida H, Kiso M, et al. The crystal structure of tetanus toxin H_C fragment complexed with a synthetic GT1b analogue suggests cross-linking between ganglioside receptors and the toxin. J Biol Chem 2001;276: 32274–81.
[21] Kohda T, Ihara H, Seto Y, Tsutsuki H, Mukamoto M, Kozaki S. Differential contribution of the residues in C-terminal half of the heavy chain of botulinum neurotoxin type B to its binding to the ganglioside GT1b and the synaptotagmin 2/GT1b complex. Microb Pathog 2007;42:72–9.
[22] Lacy DB, Tepp W, Cohen AC, DasGupta BR, Stevens RC. Crystal structure of botulinum neurotoxin type A and implications for toxicity. Nat Struct Biol 1998;5:898–902.
[23] Swaminathan S, Eswaramoorthy S. Structural analysis of the catalytic and binding sites of *Clostridium botulinum* neurotoxin B. Nat Struct Biol 2000;7:693–9.
[24] Dong M, Richards DA, Goodnough MC, Tepp WH, Johnson EA, Chapman ER. Synaptotagmins I and II mediate entry of botulinum neurotoxin B into cells. J Cell Biol 2003;162:1293–303.
[25] Nishiki T, Kamata Y, Nemoto Y, Omori A, Ito T, Takahashi M, et al. Identification of protein receptor for *Clostridium botulinum* type B neurotoxin in rat brain synaptosomes. J Biol Chem 1994;269: 10498–503.
[26] Nishiki T, Tokuyama Y, Kamata Y, Nemoto Y, Yoshida A, Sato K, et al. The high-affinity binding of *Clostridium botulinum* type B neurotoxin to synaptotagmin II associated with gangliosides GT1b/GD1a. FEBS Lett 1996;378:253–7.
[27] Dong M, Yeh F, Tepp WH, Dean C, Johnson EA, Janz R, et al. SV2 is the protein receptor for botulinum neurotoxin A. Science 2006;312:592–6.
[28] Mahrhold S, Rummel A, Bigalke H, Davletov B, Binz T. The synaptic vesicle protein 2C mediates the uptake of botulinum neurotoxin A into phrenic nerves. FEBS Lett 2006;580:2011–4.
[29] Tsukamoto K, Kohda T, Mukamoto M, Takeuchi K, Ihara H, Saito M, et al. Binding of *Clostridium botulinum* type C and D neurotoxins to ganglioside and phospholipid. Novel insights into the receptor for clostridial neurotoxins. J Biol Chem 2005;280:35164–71.
[30] Horton RM, Cai ZL, Ho SN, Pease LR. Gene splicing by overlap extension: tailor-made genes using the polymerase chain reaction. Biotechniques 1990;8:528–35.
[31] Kozaki S. Interaction of botulinum type A, B and E derivative toxins with synaptosomes of rat brain. Naunyn-Schmiedeberg's Arch Pharmacol 1979;308:67–70.
[32] Whittaker VP. The isolation and characterization of acetylcholine-containing particles from brain. Biochem J 1959;72:694–706.
[33] Ihara H, Kohda T, Morimoto F, Tsukamoto K, Karasawa T, Nakamura S, et al. Sequence of the gene for *Clostridium botulinum* type B neurotoxin associated with infant botulism, expression of the C-terminal half of heavy chain and its binding activity. Biochim Biophys Acta 2003;1625:19–26.

Please cite this article as: Tsukamoto K, et al. Identification of the receptor-binding sites in the carboxyl-terminal half of the heavy chain of botulinum neurotoxin types C and D. Microb Pathog (2008), doi:10.1016/j.micpath.2007.12.003

[34] Laemmli UK. Cleavage of structural proteins during the assembly of the head of bacteriophage T4. Nature 1970;227:680–5.
[35] Lowry OH, Rosebrough NJ, Farr AL, Randall RJ. Protein measurement with the Folin phenol reagent. J Biol Chem 1951;193:265–75.
[36] Rummel A, Bade S, Alves J, Bigalke H, Binz T. Two carbohydrate binding sites in the H_{CC}-domain of tetanus neurotoxin are required for toxicity. J Mol Biol 2003;326:835–47.
[37] Machaidze G, Seelig J. Specific binding of cinnamycin (Ro 09-0198) to phosphatidylethanolamine. Comparison between micellar and membrane environments. Biochemistry 2003;42:12570–6.
[38] Machaidze G, Ziegler A, Seelig J. Specific binding of Ro 09-0198 (cinnamycin) to phosphatidylethanolamine: a thermodynamic analysis. Biochemistry 2002;41:1965–71.
[39] Rummel A, Mahrhold S, Bigalke H, Binz T. The H_{CC}-domain of botulinum neurotoxins A and B exhibits a singular ganglioside binding site displaying serotype specific carbohydrate interaction. Mol Microbiol 2004;51:631–43.
[40] Halpern JL, Loftus A. Characterization of the receptor-binding domain of tetanus toxin. J Biol Chem 1993;268:11188–92.

Please cite this article as: Tsukamoto K, et al. Identification of the receptor-binding sites in the carboxyl-terminal half of the heavy chain of botulinum neurotoxin types C and D. Microb Pathog (2008), doi:10.1016/j.micpath.2007.12.003